ELSEVIER

Journal of Nuclear Materials 295 (2001) 233–243

journal of nuclear materials

www.elsevier.nl/locate/jnucmat

Effect of electrolyte composition on the electrochemical potentiokinetic reactivation behavior of Alloy 600

Tsung-Feng Wu [a], Tzu-Ping Cheng [b], Wen-Ta Tsai [a,*]

[a] *Department of Materials Science and Engineering, National Cheng Kung University, Tainan 70101, Taiwan, ROC*
[b] *Materials Research Laboratories, Industrial Technology Research Institute, Hsinchu, Taiwan, ROC*

Received 7 December 2000; accepted 8 March 2001

Abstract

The effects of electrolyte composition and concentration on the reactivation behavior of Alloy 600 in H_2SO_4 + KSCN solution were investigated by conducting single-loop electrochemical potentiokinetic reactivation (SL-EPR) tests. The experimental results revealed that two anodic peaks existed, which corresponded to pitting corrosion and matrix corrosion, respectively, in the reactivation polarization curve of non-sensitized Alloy 600. Alternately, for sensitized Alloy 600, an additional peak associated with grain boundary corrosion appeared in the potential range of +60 to −10 mV_{SCE} within the reactivation polarization curve. The shape and current density of the reactivation curve of Alloy 600 with different degrees of sensitization varied with the electrolyte composition adjustments. A maximum peak anodic current density associated with grain boundary corrosion occurred when the concentration ratio of H_2SO_4/KSCN was 10 for the sensitized low carbon Alloy 600.

1. Introduction

Electrochemical potentiokinetic reactivation (EPR) technique for passivated stainless steel was proposed in the 1960s as a method to detect stainless steel's susceptibility to intergranular attack (IGA) [1–3]. The susceptibility was produced by chromium depletion in the vicinity of the grain boundaries, which resulted from chromium carbide precipitation of numerous stainless steels following welding operations and other thermal exposures between 500°C and 800°C [4,5]. The chromium content in these depleted regions was considerably lower than that of the undepleted grain matrix. Therefore, these depleted regions might be subject to rapid preferential attack. The reactivation technique was developed further into a quantitative, non-destructive testing method for measuring sensitization in welded austenitic stainless steels (such as 304 and 304 L piping) for use in a boiling water reactor (BWR) nuclear reactor plants [6–8]. To date, the EPR technique, proposed by Prazak [1] and Clarke et al. [6,8], then developed by Novak [3] and others [2,9,10], has become the standard method to detect the degrees of sensitization in austenitic stainless steels. The magnitudes of Pa and I_a/I_p ratio are commonly used to evaluate the degree of sensitization. The Pa value is the integrated charge of the reactivation curve divided by the grain boundary area in single loop EPR (SL-EPR) test [11]. In the double-loop EPR (DL-EPR) test, the peak current density ratio I_a/I_p, where I_a is the maximum current density in the reversed reactivation scan and I_p is the critical passivation current density in the forward scan, is used as a criterion [12]. The electrolyte selected was normally an H_2SO_4+KSCN solution of varying concentrations.

High nickel alloys, such as Alloy 600 and Alloy 690, were developed for use in heat exchangers and various elements of pressurized water reactors (PWRs) based on their excellent corrosion behavior in simulated primary and secondary reactor water environments. However, it has also been proposed that Alloy 600 is susceptible to intergranular stress corrosion cracking (IGSCC) and IGA when the grain boundary Cr level is below approximately 8 wt% in caustic water solutions [13]. For the reason, it is essential to develop the non-destructive

* Corresponding author. Fax: +886-6 275 4395.
E-mail address: wttsai@mail.ncku.edu.tw (W.-T. Tsai).

0022-3115/01/$ - see front matter
PII: S0022-3115(01)00558-X

Table 1
Chemical composition (wt%) of Alloy 600 used

Element	Fe	Ni	Cr	C	Si	Mn	Cu	S
wt%	Bal.	74.55	16.19	0.023	0.25	0.31	0.19	0.002

and rapid method to detect the degree of sensitization for Alloy 600.

The EPR test technique also has been applied to evaluate the susceptibility of high-nickel alloys to intergranular corrosion [14–16]. However, Vereecken et al. [14] demonstrated that the SL-EPR curve of Alloy 600 contained more than one peak in $H_2SO_4 + KSCN$ electrolyte. Microstructural analysis revealed that the peak at -30 mV_{SCE} corresponded to IGA, and the peak at -150 mV_{SCE} corresponded to a pitting-like attack. In addition, Edgemon et al. [16] also discovered that the reactivation curve, which was absent for a solution annealed 304 SS, existed even in the non-sensitized nickel base Alloy 800H (mill-annealed 1150°C for 1 h). EPR curve with dual peaks was found for the sensitized Alloy 800H. In our recent investigation [17], similar results also were obtained, indicating that reactivation peaks were found for either sensitized or non-sensitized low carbon content (0.023 wt%) Alloy 600 in 0.5 M H_2SO_4 + 0.005 M KSCN solution. The EPR curve could be dissociated into two parts with one that corresponded to the grain matrix depassivation and the other, which corresponded to grain boundary or localized corrosion. Fig. 1 depicts a schematic diagram of the EPR curve deconvolution for Alloy 600 in 0.5 M H_2SO_4 + 0.005 M KSCN solution. All these investigations indicated that the EPR method, although valid for austenitic stainless steels in evaluating the degree of sensitization, might not be applied to nickel base alloys due to the additional electrochemical reaction that is involved in the reactivation process [14,16–18].

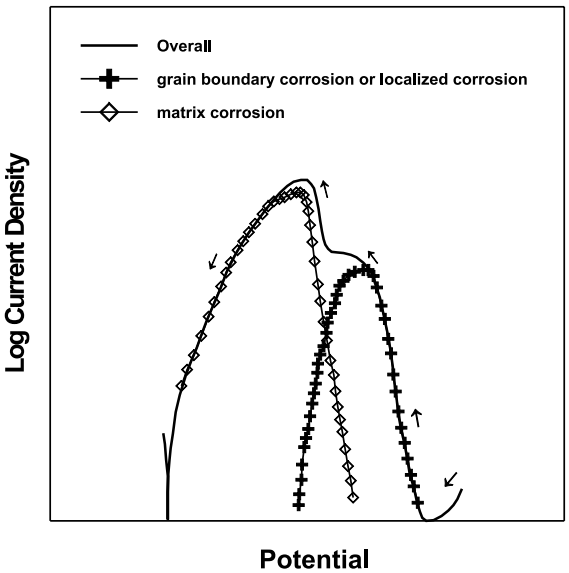

Fig. 1. Schematic diagram illustrating the deconvolution of the EPR curve for Alloy 600 in 0.5 M H_2SO_4 + 0.005 M KSCN solution.

Furthermore, it has been found that the reactivation behavior varied with the composition of electrolyte employed [14]. However, whether the EPR method is valid to detect the sensitization degree of nickel base alloys by varying the electrolyte composition remains vague. Thus, in this investigation, the reactivation behavior of Alloy 600 in the $H_2SO_4 + KSCN$ electrolytes with various concentrations is explored. Furthermore, the specific reactions associated with the reactivation process in H_2SO_4/KSCN electrolytes also are investigated.

2. Experimental

Table 1 lists the chemical composition of the mill-annealed Alloy 600 provided by Sumitomo Metal Technology. To facilitate subsequent tests, the mill-annealed Alloy 600 plate was cut into several $10 \times 10 \times 2$ mm^3 specimens. They were then all solution-treated at 1150°C for 1 h, which was followed by water quenching to prevent carbide precipitation in the matrix. To simulate the non-uniform heat distributions in Alloy 600 during the welding procedure, two alternate thermal treatments were applied. Table 2 indicates that after solution annealing (1150°C/1 h + water quench), specimens A and B were treated for 1 h at 1024°C and 15 h at 704°C, they were then water-quenched, respectively. Following heat treatment, the specimens were ground with silicon carbide paper to a 2000 grit finish, polished with 1 μm alumina particles, and rinsed in

Table 2
Heat treatments applied to Alloy 600

Specimen designation	Heat treatment
Solution annealed (SA)	1150°C/1 h + water quench
Specimen A	SA + 1024°C/1 h + water quench
Specimen B	SA + 704°C/15 h + water quench

Table 3
Conditions for grain boundary and carbide etching for Alloy 600

	Grain boundary etching	Carbide etching
Electrolyte	5% HNO_3 + 95% CHOH	H_3PO_4:H_2O = 8:1
Applied potential	+3 V	+3 V
Reference eletrode	Pt	Pt
Etching time	50 s	20 s

distilled water prior to metallographical, chemical and electrochemical tests. In metallographical examinations, two distinct etching procedures, one to reveal grain boundaries and the other carbides, were employed. Table 3 displays the electrolytes and etching conditions for these two procedures. Herein, the modified Huey test [19–21] (in boiling 25% HNO_3 solution) was employed to examine the degree of sensitization in Alloy 600 with varying thermal treatments. Weight loss of each specimen was measured following 48 h immersion in the boiling solution. Following the test, the surface morphology of the specimen was then examined via scanning electron microscopy (SEM).

To examine the effect of electrolyte concentration on the reactivation polarization behavior, the mixed solutions of H_2SO_4/KSCN with various compositions were employed (Table 4). Reactivation polarization behaviors of Alloy 600 within these electrolytes were evaluated via the SL-EPR test. Each specimen was first held at +400 mV_{SCE} for 120 s to form a passive film on the surface. Then, the potential of the specimen was swept from +400 to −375 mV, at a potential scan rate of 1.67 mV/s. Thus, the reactivation polarization curve was determined. Table 5 lists the detailed conditions for the EPR test. All of the potentials in this study were measured with respect to a saturated calomel electrode (SCE). Subsequent to each EPR test, the specimen was examined using optical microscopy. A reactivation termination test also was performed on some specimens. The procedure was identical to the SL-EPR test except that the potential was scanned to and terminated at a specific predeterminated potential. Following each potential scan termination test, the specimen was examined metallographically.

Table 4
Electrolyte compositions employed for SL-EPR test

H_2SO_4 (M)	KSCN (M)	H_2SO_4/KSCN
0.5	0.5	1/1
0.5	0.05	10/1
0.5	0.005	100/1
0.1	0.01	10/1
0.05	0.05	1/1
0.05	0.005	10/1
0.005	0.005	1/1

Table 5
Parameters employed for SL-EPR test for Alloy 600

Electrolyte	
Acid concentration	0.005–0.5 M H_2SO_4
KSCN concentration	0.005–0.5 M
Temperature	25°C
Passivation	
Potential	+400 mV_{SCE}
Time	120 s
Reactivation	
Potential range	+400 → −375 mV_{SCE}
Scan rate	1.67 mV/s

3. Results and discussions

3.1. Microstructure examination

Figs. 2 and 3 depict the optical micrographs of Alloy 600 with various thermal treatments. Fig. 2 presents the photomicrographs for the specimens that were etched electrolytically in 5% HNO_3 + 95% CH_3OH solution to reveal the grain boundaries. The experimental results demonstrated that both the specimens exhibited equiaxied grains with an average size of 200 μm. The results indicated that grain size was determined by the solution annealing treatment, not affected by the subsequent heat treatment.

Fig. 3 demonstrates micrographs for the specimens that were etched in H_3PO_4/H_2O solution. The experimental results revealed that carbide precipitation was negligible for Alloy 600 that was heat-treated at 1024°C/1 h following solution annealing (specimen A). Extensive grain boundary carbide precipitation, however, was observed for the specimen heat-treated at 704°C/15 h (specimen B). Although the carbon content of the alloy used was merely 0.023 wt%, carbide precipitation at grain boundaries was significant in specimen B.

3.2. Modified Huey test

The weight loss rates of the specimens following the modified Huey test were 0.066 g/cm^2 h for specimen A and 0.580 g/cm^2 h for specimen B, respectively. Notably, a higher weight loss rate occurred in the specimen that was heat-treated at 704°C/15 h (specimen B), which was related to grain boundary carbide precipitation. Fig. 4 demonstrates SEM micrographs for Alloy 600, following modified Huey tests with different heat

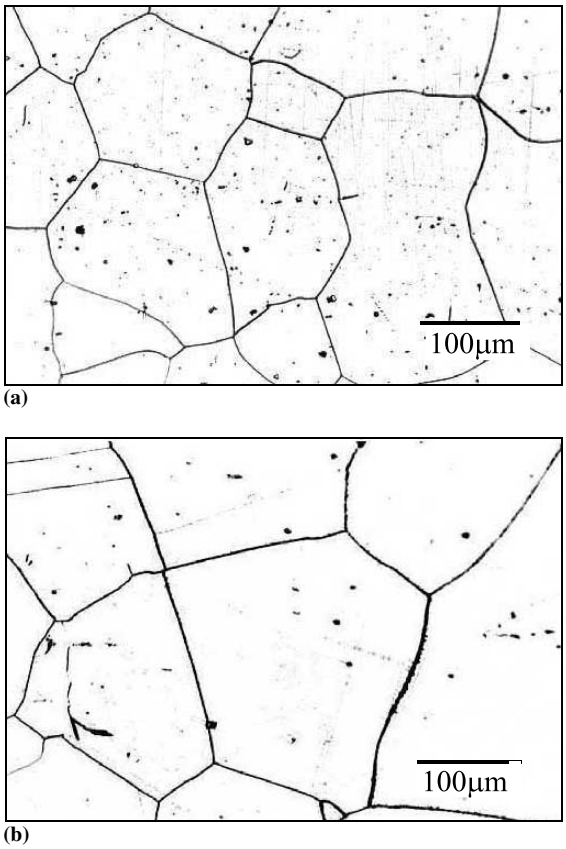

Fig. 2. Microstructures of Alloy 600 with different thermal treatments, etched electrolytically in 5% HNO_3 + 95% CHOH: (a) specimen A (SA + 1024°C/1 h); (b) specimen B (SA + 704°C/15 h).

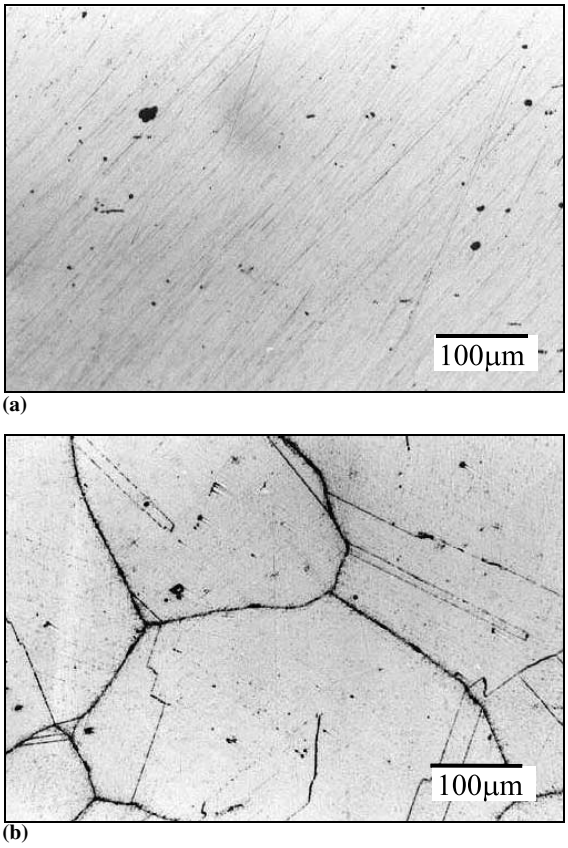

Fig. 3. Photomicrographs depicting carbide precipitation of Alloy 600 with different thermal treatments, electrolytically etched in H_3PO_4:H_2O = 8:1 electrolyte: (a) specimen A (SA + 1024°C/1 h); (b) specimen B (SA + 704°C/15 h).

treatments. Specimen A did not reveal intergranular corrosion. Fig. 4(a) shows pits, which were associated with the presence of TiN that formed in the specimen. For the specimen heat-treated at 704°C/15 h following solution annealing at 1150°C/1 h (specimen B), grains dropped out of the surface, which resulted from grain boundary corrosion (Fig. 4(b)). The experimental results indicate that specimen A was not sensitized, while specimen B was sensitized and susceptible to intergranular corrosion. Clearly these two heat treatments resulted in varying degrees of sensitization of Alloy 600.

3.3. Single-loop electrochemical potentiokinetic reactivation

Fig. 5(a) illustrates the SL-EPR polarization curves of Alloy 600 with various heat treatments, which were conducted in 0.5 M H_2SO_4 + 0.005 M KSCN solution. Notably, regardless of the heat treatment, a hump appeared in each reactivation polarization curve. This differs significantly from that, which occurs in stainless steel where no reactivation hump was discovered for the non-sensitized alloy. Basically, the reactivation curve shapes of the two alternate thermally treated Alloy 600 specimens were almost identical. However, surface morphologies of these two specimens following SL-EPR tests, presented in Figs. 5(b) and (c), respectively, were apparently different. Although pits were discovered on surfaces of both specimens A and B, grain boundary etching occurred only on specimen B. As the modified Huey test results indicated, specimen B was susceptible to intergranular corrosion. The post metallographical examination for the SL-EPR test also demonstrated that grain boundary etching occurred in the specimen that had a high degree of sensitization (specimen B). Hence, if proper conditions were chosen, SL-EPR might be applied to differentiate the degree of sensitization for Alloy 600.

Fig. 5 depicts that two distinct peaks existed in each of the reactivation curves. According to the experimental results of a previous investigation [17], grain

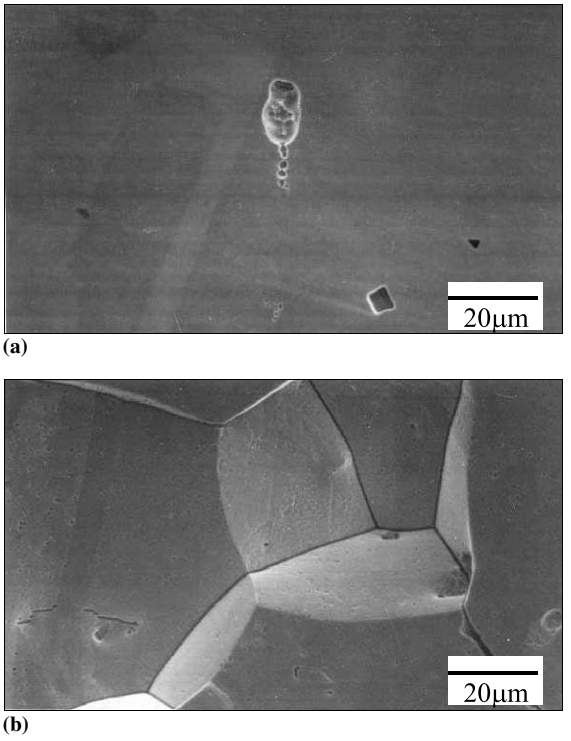

Fig. 4. SEM micrographs revealing the surface appearances of Alloy 600 with different thermal treatments following the modified Huey test: (a) specimen A (SA + 1024°C/1 h); (b) specimen B (SA + 704°C/15 h).

boundary or localized corrosion produced the first peak at high anodic potential and grain matrix corrosion produced the second, which was at a lower potential (Fig. 1). The metallographical results depicted in Figs. 5(b) and (c) supported this viewpoint, except that the peaks do not distinguish between pitting corrosion and grain boundary corrosion. Thus, to determine whether pitting corrosion and grain boundary corrosion could be differentiated, the electrolyte composition was altered.

3.3.1. Influence of KSCN concentration

Previous investigations have indicated that in the electrolyte, which is employed in the EPR test, KSCN is added as the depassivating agent [1,2,14]. The depassivating effect, which is a function of KSCN concentration, is dependent on the passive film properties. Figs. 6(a) and 7(a) depict the single loop reactivation curves of Alloy 600 with various thermal treatments in 0.5 M H_2SO_4 solution with 0.05 and 0.5 M KSCN, respectively. These curves exhibited large reactivation humps, which consisted of two or more anodic peaks. Compared to the reactivation curve presented in Fig. 5(a), the relative intensities of the first and the second peaks varied with the KSCN concentration. Evidentially, as the KSCN concentration increased, the intensity of the second peak decreased more than that of the first one. Furthermore, when 0.05 M KSCN was present

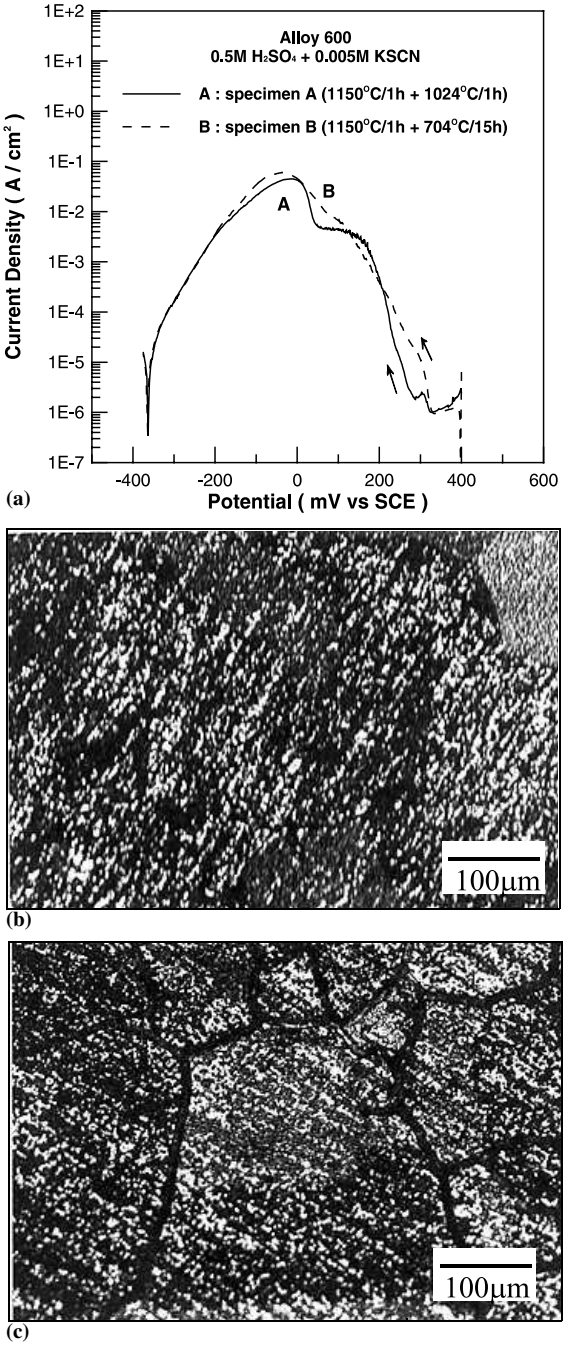

Fig. 5. Polarization curves and optical micrographs of Alloy 600 with different thermal treatments following SL-EPR tests in 0.5 M H_2SO_4 + 0.005 M KSCN solution, (a) polarization curves, and optical micrographs for (b) specimen A (SA + 1024°C/1 h) and (c) specimen B (SA + 704°C/15 h).

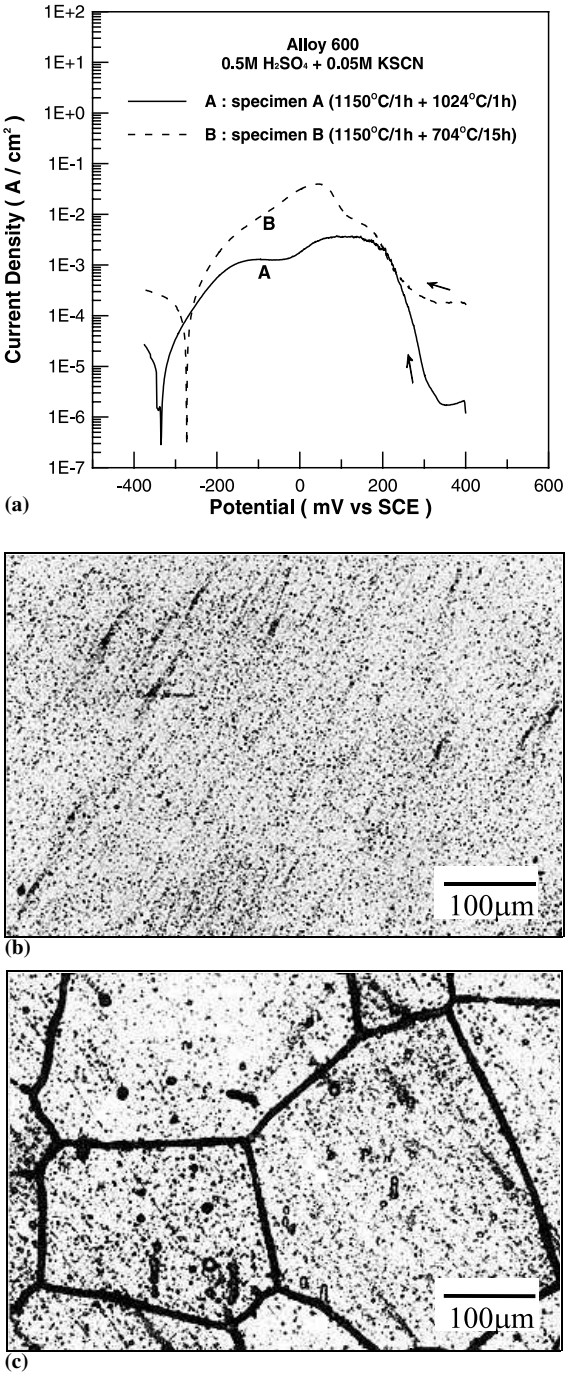

Fig. 6. Polarization curves and optical micrographs of Alloy 600 with different thermal treatments following SL-EPR tests in 0.5 M H_2SO_4 + 0.05 M KSCN solution: (a) polarization curves, and optical micrographs for (b) specimen A (SA + 1024°C/1 h) and (c) specimen B (SA + 704°C/15 h).

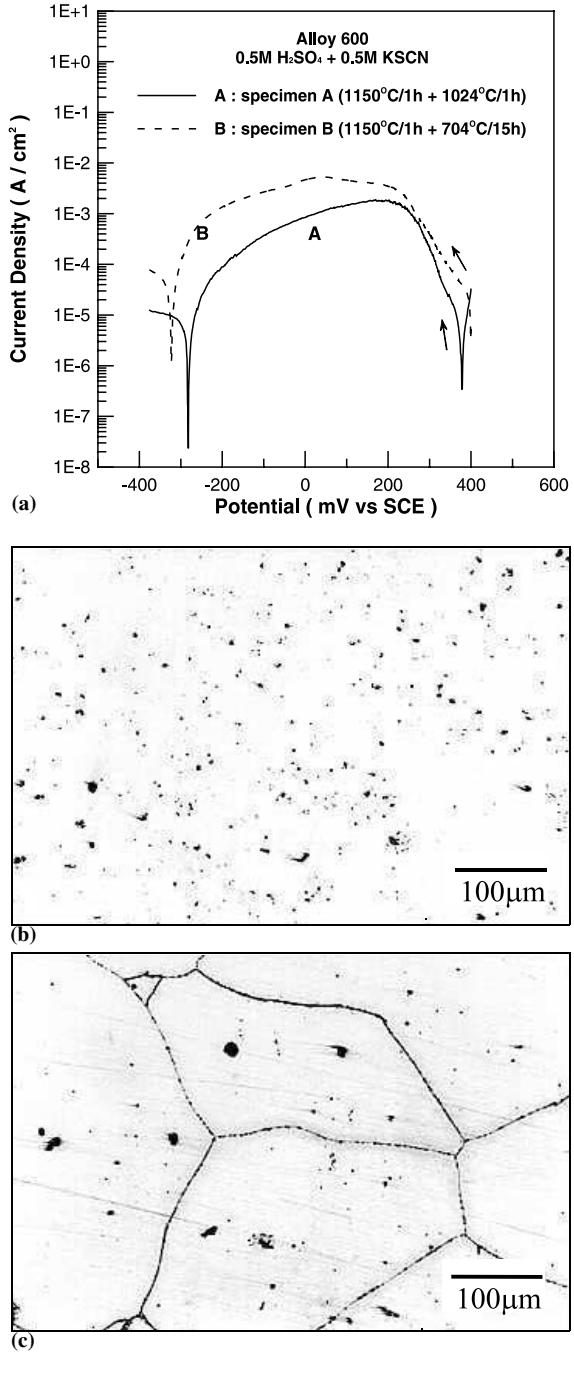

Fig. 7. Polarization curves and optical micrographs of Alloy 600 with different thermal treatments following SL-EPR tests in 0.5 M H_2SO_4 + 0.5 M KSCN solution: (a) polarization curves, and optical micrographs for (b) specimen A (SA + 1024°C/1 h) and (c) specimen B (SA + 704°C/15 h).

in the electrolyte, three peaks (at +150, +50 and −100 mV) appeared in the reactivation curve of the sensitized Alloy 600 (Fig. 6(a)). At 0.5 M KSCN, the differences among the peaks became almost indistinguishable. However, post EPR metallographical examination continued to reveal the difference in the degree of sensiti-

zation. The micrographs presented in Figs. 6(b) and (c), and 7(b) and (c), clearly demonstrate that grain boundary corrosion only occurred in the sensitized Alloy 600. Namely, the EPR test can differentiate the degree of sensitization of Alloy 600. Fig. 6(c) depicts that pronounced intergranular corrosion occurred when 0.5 M $H_2SO_4 + 0.05$ M KSCN electrolyte was used, which might be associated with the third peak (+50 mV) in the reactivation curve of Fig. 6(a). The respective reactivation peaks that appeared in curve B of Fig. 6(a) will be further discussed later.

It has been indicated that for sensitized nickel base alloys, one of the reactivation peaks (at higher anodic potential) was produced by grain boundary corrosion [14–17]. Roelandt and Vereecken [14] indicated that, in the KSCN range of 20–200 ppm, the maximum current density that corresponded to intergranular corrosion of sensitized Alloy 600 in 1 N H_2SO_4 solution increased with an increasing KSCN concentration. Clearly, the EPR resolution to detect the degree of sensitization within Alloy 600 was a function of KSCN concentration. At a higher KSCN concentration, the contribution of reactivation current density from the depassivated matrix became prominent. As a result, the discriminating power for the degree of sensitization of EPR in H_2SO_4/KSCN electrolyte was decreased. For the low carbon Alloy 600 studied herein, similar results occurred. However, the maximum resolution was discovered in the 0.5 M H_2SO_4 electrolyte that contained a much higher KSCN concentration (approximately 0.05 M). Actually, the anodic peak which was associated with the intergranular corrosion was the middle (at +50 mV) of the three peaks that appeared in Fig. 6(a). The maximum current density of the middle peak also increased with an increase in KSCN concentration from 0.005 to 0.05 M. However, as the KSCN concentration was increased to 0.5 M, it then decreased.

3.3.2. Influence of H_2SO_4 concentration

The influence of H_2SO_4 concentration on the reactivation behavior of Alloy 600 within the electrolyte that contained 0.005 M KSCN was examined. Figs. 8 and 9 demonstrate the EPR curves and the corresponding micrographs for sensitized and non-sensitized Alloy 600 in 0.05 M $H_2SO_4 + 0.005$ M KSCN and 0.005 M $H_2SO_4 + 0.005$ M KSCN electrolytes, respectively. Basically, the EPR curves obtained in the electrolytes with 0.05 and 0.005 M H_2SO_4 were similar to those depicted in Fig. 5(a). However, the anodic current densities that were determined decreased with a decrease in H_2SO_4 concentration. As compared to that at 0.5 M H_2SO_4, the differences in the anodic current density magnitudes were pronounced for the sensitized and non-sensitized Alloy 600 in the electrolytes containing 0.05 and 0.005 M H_2SO_4.

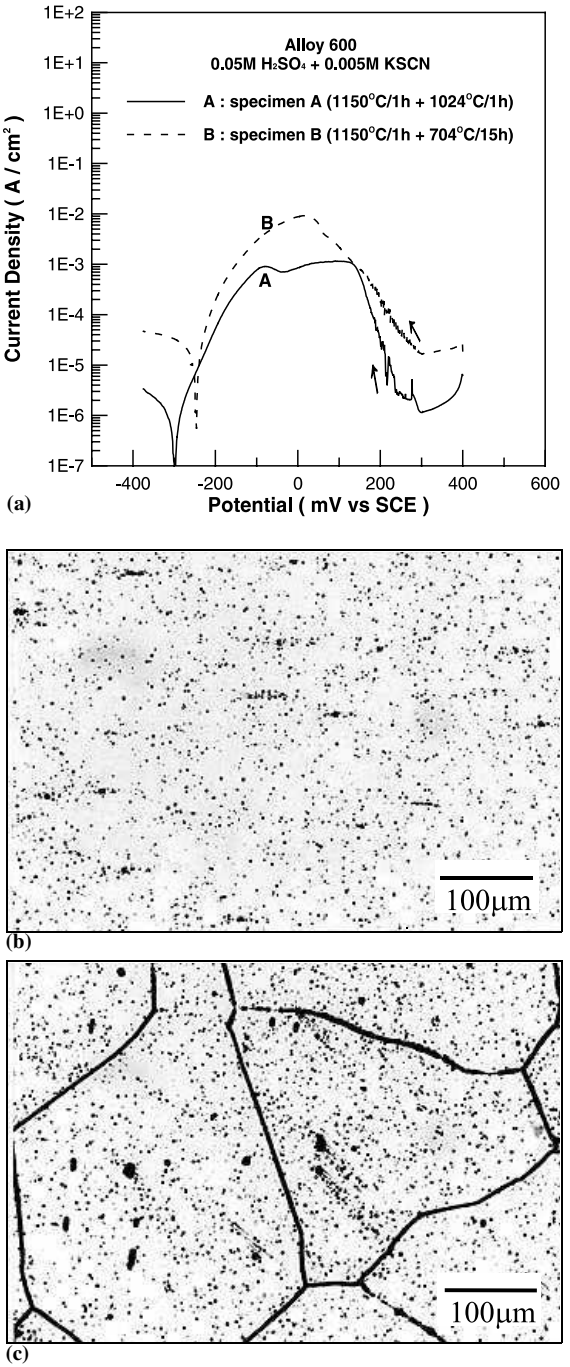

Fig. 8. Polarization curves and optical micrographs of Alloy 600 with different thermal treatments following SL-EPR tests in 0.05 M $H_2SO_4 + 0.005$ M KSCN solution: (a) polarization curves, and optical micrographs for (b) specimen A (SA + 1024°C/1 h) and (c) specimen B (SA + 704°C/15 h).

Metallographical examinations indicated that non-sensitized Alloy 600 did not reveal intergranular corrosion following EPR tests (Figs. 8(b) and 9(b)). However,

pitting corrosion continued to exist in each specimen tested in either 0.05 $H_2SO_4 + 0.005$ M KSCN or 0.005 M $H_2SO_4 + 0.005$ M KSCN electrolyte. Alternately, intergranular corrosion was observed for the sensitized Alloy 600 within these two electrolytes (Figs. 8 and 9). The extent of intergranular corrosion was more pronounced in the electrolyte that contained 0.05 M H_2SO_4. Notably, the peak at +50 mV was the highest, as the concentration of H_2SO_4 was 0.05 M, where grain boundary corrosion was more distinct. These experimental results clearly indicate that both KSCN and H_2SO_4 concentrations affected the EPR behavior of Alloy 600. Seemingly, the discriminating power to detect grain boundary corrosion of sensitized Alloy 600 was dependent on the concentration ratio of H_2SO_4/KSCN, which will be discussed in the following section.

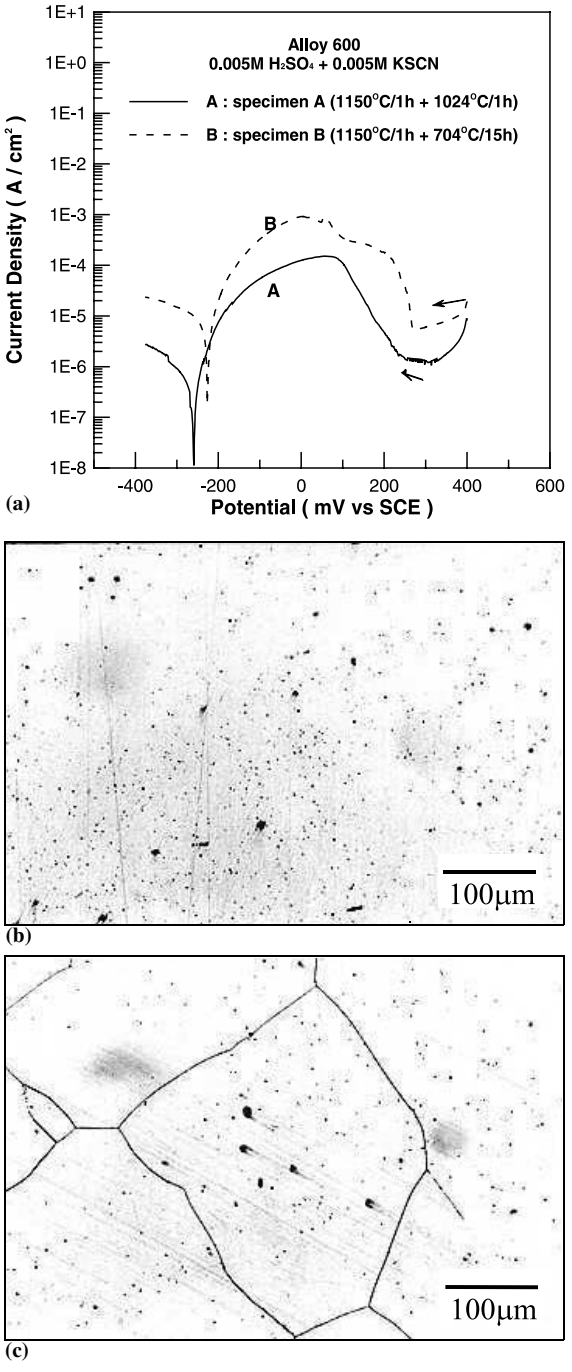

Fig. 9. Polarization curves and optical micrographs of Alloy 600 with different thermal treatments following SL-EPR tests in 0.005 M $H_2SO_4 + 0.005$ M KSCN solution: (a) polarization curves, and optical micrographs for (b) specimen A (SA + 1024°C/1 h) and (c) specimen B (SA + 704°C/15 h).

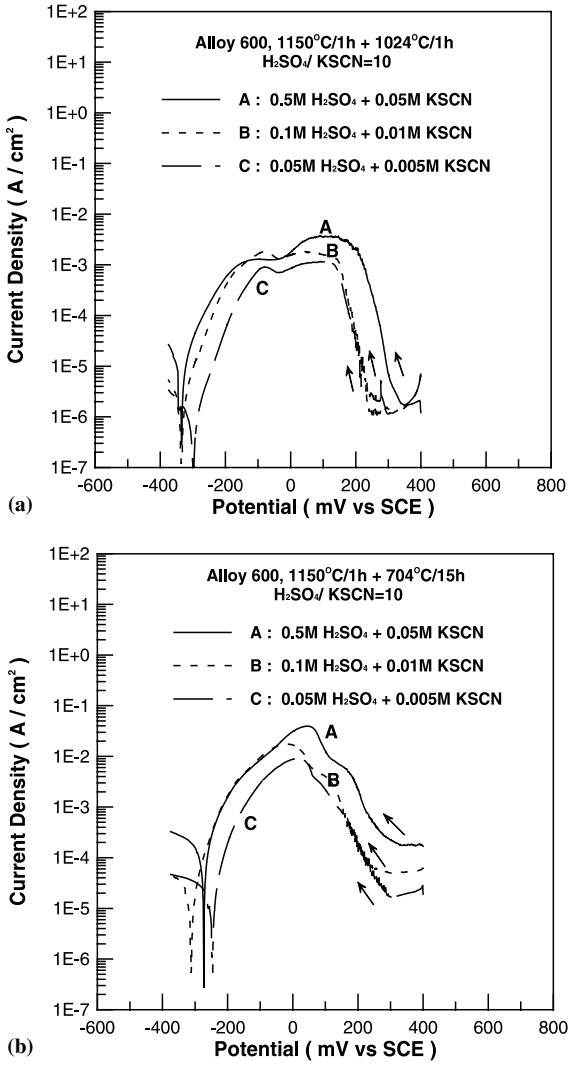

Fig. 10. Polarization curves of Alloy 600 with different thermal treatments following SL-EPR tests in solution, which contained H_2SO_4:KSCN = 10:1 (a) specimen A (SA + 1024°C/1 h); (b) specimen B (SA + 704°C/15 h).

3.3.3. Influence of H_2SO_4/KSCN ratio

Figs. 6 and 8 depict that the susceptibility to grain boundary corrosion was easily identifiable when the concentration ratio of H_2SO_4/KSCN was 10. Further EPR tests in the electrolytes with various compositions but with a H_2SO_4/KSCN ratio of 10, were conducted. Fig. 10 depicts the experimental results for non-sensitized Alloy 600 (Fig. 10(a)), in which two anodic peaks continued to exist in the reactivation curves within the various electrolytes. Post metallographical examination

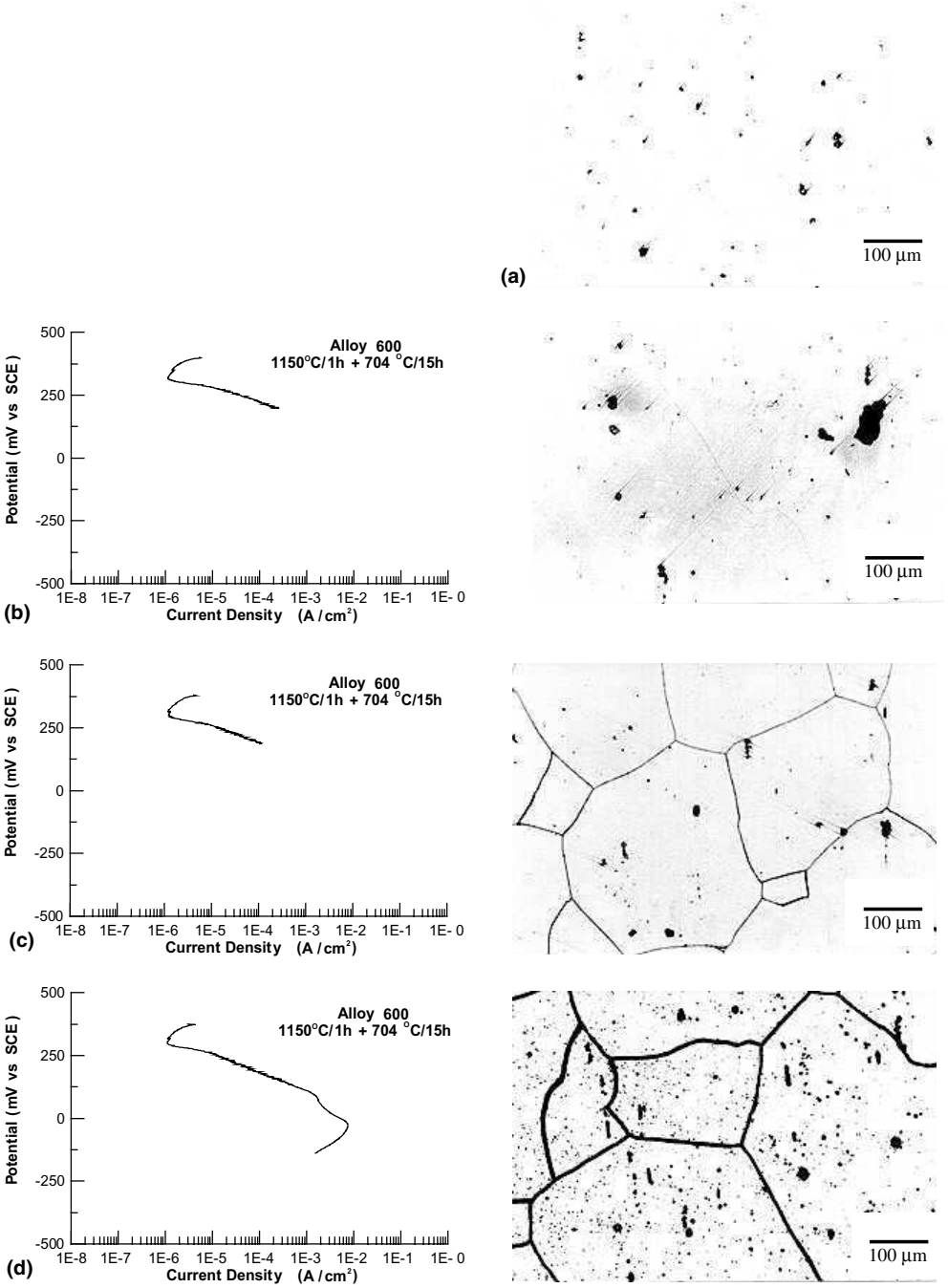

Fig. 11. Comparison of polarization curves and surface micrographs of specimen B (SA + 704°C/15 h) for reactivation termination tests at varying potentials in 0.1 M H_2SO_4 + 0.01 M KSCN solution: (a) prior to test, (b) +200 mV_{SCE}, (c) +60 mV_{SCE}, (d) −130 mV_{SCE}.

revealed only matrix and pitting corrosion, and no grain boundary corrosion. As stated previously, the first peak at a higher potential corresponded to the occurrence of pitting corrosion, and the later at a lower anodic potential to the matrix corrosion.

For each specimen of sensitized Alloy 600, which was tested in the electrolytes with a H_2SO_4/KSCN ratio of 10 (Fig. 10(b)), an additional peak appeared in the potential range of +60 to −10 mV. Moreover, this peak had the maximum anodic current density within each curve. Reactivation termination tests were further conducted upon the sensitized Alloy 600 in the 0.1 M H_2SO_4+ 0.01 M KSCN electrolyte. Fig. 11 demonstrates the experimental results. Fig. 11(a) depicts the etched micrograph of the sensitized material prior to the EPR test. Inclusions, primarily TiN, existed on the surface of the specimen. After sweeping the potential from +400 mV towards the cathodic direction and terminating at +200 mV, the resulting microstructure revealed only pitting corrosion around the inclusions (Fig. 11(b)). Alternately, when the reactivation was terminated at +60 mV, grain boundary corrosion was evident on the surface of the sensitized Alloy 600 (Fig. 11(c)). Clearly, the peak that appeared in the reactivation polarization curve at the potential in the range of +60 to −10 mV was associated with grain boundary corrosion. When the potential was terminated at −130 mV, matrix corrosion became noticeable (Fig. 11(d)). This experimental result indicated that the anodic peak at −100 mV, as demonstrated in Fig. 11(d), was associated primarily with matrix corrosion, which increased with an increase in H_2SO_4 concentration.

By increasing the H_2SO_4/KSCN ratio to 100, the peak associated with matrix corrosion increased and became the highest peak in the reactivation polarization curve. Furthermore, at this concentration ratio, the corresponding peaks for grain boundary corrosion and pitting corrosion were not distinguishable. In contrast, at a H_2SO_4/KSCN concentration ratio of 1, the matrix corrosion peak decreased. Although three anodic peaks were observed, the difference in peak intensities between grain boundary corrosion and pitting corrosion was not significant. Therefore, the EPR curve could not properly differentiate between these reactivation reactions for sensitized Alloy 600 in the electrolyte with a H_2SO_4/KSCN concentration ratio of 1.

Based on the above observations, the EPR test might be applied to detect the degree of sensitization for Alloy 600 only if the electrolyte is chosen properly. For the low carbon Alloy 600 employed herein, the electrolyte with a H_2SO_4/KSCN ratio of 10 was the most sensitive. As well, the respective concentrations of H_2SO_4 and KSCN, in the range of 0.005–0.5 M, also were essential.

At the H_2SO_4/KSCN ratio of 10, the reactivation polarization curves were dissociated into two or three partial reactions depending on whether Alloy 600 was sensitized or not. Fig. 12 illustrates a schematic diagram, which indicates that the reactivation polarization curve consisted of pitting corrosion at relative higher anodic potential and matrix corrosion at lower anodic potential within the annealed or non-sensitized Alloy 600 solution. For sensitized Alloy 600, an intermediate peak with the highest anodic current density existed in the deconvolution diagram (Fig. 12).

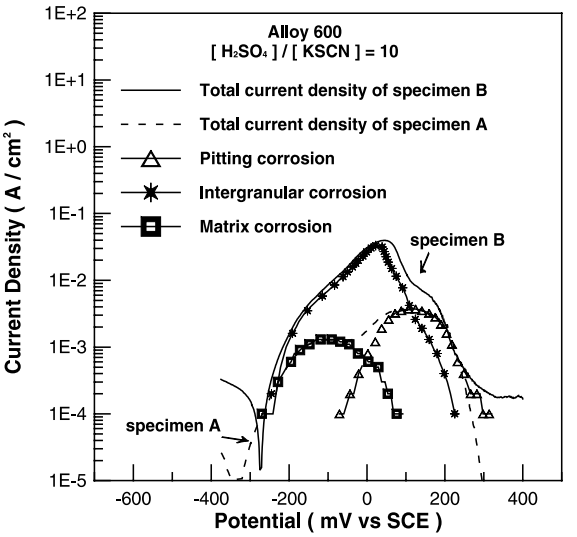

Fig. 12. Deconvolution diagram of the reactivation polarization curves of Alloy 600 with different thermal treatments in 0.5 M H_2SO_4 + 0.05 M KSCN (H_2SO_4:KSCN = 10:1) solution.

4. Conclusions

1. For non-sensitized Alloy 600, two anodic peaks existed in the reactivation polarization curve in H_2SO_4/KSCN electrolytes. These two anodic peaks corresponded to pitting corrosion at a higher anodic potential and matrix corrosion at a lower potential.
2. For sensitized Alloy 600, three anodic peaks appeared in the reactivation polarization curve in H_2SO_4/KSCN electrolyte. The anodic peak that appeared in the potential range of +60 to −10 mV_{SCE} was associated with grain boundary corrosion.
3. The H_2SO_4 and KSCN concentrations within the electrolyte determined the relative intensities of the three anodic peaks in the reactivation polarization curve of sensitized Alloy 600. The maximum anodic peak associated with grain boundary corrosion occurred when the H_2SO_4/KSCN concentration ratio was 10 and the H_2SO_4 and KSCN concentrations ranged from 0.005 to 0.5 M.

Acknowledgements

The authors would like to thank the Materials Research Laboratory, the Industrial Technology Research Institute (ITRI), Taiwan, for their financial support of this research.

References

[1] M. Prazak, Corrosion 19 (3) (1963) 75.
[2] F. Duffaut, J.P. Pouzet, P. Lacombe, Corros. Sci. 6 (1966) 83.
[3] P. Novak, R. Stefec, F. Franz, Corrosion 31 (10) (1975) 344.
[4] R.L. Cowan, C.S. Tedmon Jr., Adv. Corros. Sci. Technol. 3 (1973) 293.
[5] C.S. Pande, M. Suenaga, B. Vyas, H.S. Isaacs, D.F. Harling, Scr. Metall. 11 (1977) 681.
[6] W.L. Clarke, R.L. Cowan, W.L. Walker, in: R.F. Steigerwald (Ed.), Intergranular Corrosion of Stainless Alloys, ASTM STP 656, ASTM, Philadelphia, PA, 1978, p. 99.
[7] B. Vyas, H.S. Issacs, in: R.F. Steigerwald (Ed.), Intergranular Corrosion of Stainless Alloys, ASTM STP 656, ASTM, Philadelphia, PA, 1978, p. 133.
[8] W.L. Clarke, D.C. Carlson, MP. 19 (3) (1980) 16.
[9] N.B. Gegelova, Zashch. Met. 8 (4) (1972) 420.
[10] L.A. Medvedeva, V.M. Knyazheva, Ya.M. Kolotyrkin, S.G. Babich, Zashch. Met. 11 (4) (1975) 699.
[11] Annual Book of ASTM Standards G 108, ASTM, Philadelphia, PA, 1994, p. 450.
[12] Annual Book of JIS Standards G 0580, JIS, Tokyo, Japan, 1993.
[13] G.S. Was, Corrosion 46 (4) (1988) 319.
[14] A. Roelandt, J. Vereecken, Corrosion 42 (5) (1986) 289.
[15] A. Mignone, A. Borello, A. La Barbera, Corrosion 38 (7) (1982) 390.
[16] G.L. Edgemon, M. Marek, D.F. Wilson, G.E.C. Bell, Corrosion 50 (12) (1994) 912.
[17] T.F. Wu, T.P. Cheng, W.T. Tsai, Mater. Chem. Phys. 70 (2001) 208.
[18] M.F. Maday, A. Mignone, M. Vittori, Corros. Sci. 28 (9) (1988) 887.
[19] G.P. Airey, A.R. Vaia, N. Pessall, R.G. Aspden, J. Met. 33 (11) (1981) 28.
[20] E.L. Hall, C.L. Briant, Metall. Mater. Trans. 16A (1985) 1225.
[21] D.R. Johns, F.R. Beckitt, Corros. Sci. 30 (2) (1990) 223.